Preparations, Structures, and Properties of Sulfato-Bridged Dinuclear and Tetranuclear Vanadium(III) Complexes with a Dinucleating Ligand, 2-Oxo-*N*,*N*′-bis(2-pyridylmethyl)-1,3-propanediamine-*N*,*N*′-diacetate

Kan Kanamori,*[1] Naoto Matsui,[1] Kentaro Takagi,[1] Yoshitaro Miyashita,[2] and Ken-ichi Okamoto[2]

[1]Department of Chemistry, Faculty of Science, University of Toyama, 3190 Gofuku, Toyama 930-8555

[2]Department of Chemistry, Graduate School of Pure and Applied Sciences, University of Tsukuba, 1-1-1 Tennodai, Tsukuba 305-8571

Received May 8, 2006; E-mail: kanamori@sci.u-toyama.ac.jp

New dinuclear and tetranuclear vanadium(III) complexes with sulfato bridge(s), $[\{V^{III}(H_2O)\}_2(\mu\text{-hpnbpda})(\mu\text{-OH})(\mu\text{-SO}_4)]\cdot 5.25H_2O$ (**1**) and $[V^{III}{}_4(\mu\text{-hpnbpda})_2(\mu\text{-OH})_2(\mu\text{-SO}_4)_2]\cdot 12H_2O$ (**2**), where hpnbpda is an alkoxo-bridging dinucleating ligand, 2-oxo-*N*,*N*′-bis(2-pyridylmethyl)-1,3-propanediamine-*N*,*N*′-diacetate, were prepared, and their structures were determined by X-ray crystallography. The vanadium(III) center in **1** adopts heptacoordinate structure while that in **2** has a hexacoordinate structure. In **2**, the two dinuclear vanadium(III) units bridged by the alkoxo group of hpnbpda are further linked by two hydroxo and two sulfato bridging groups, resulting in a dimer-of-dimers structure. Measurement of the temperature dependence of the magnetic susceptibility of **1** revealed that the two vanadium(III) ions are antiferromagnetically coupled with $J = -5.9\,cm^{-1}$ and $g = 1.90$.

Interest in vanadium chemistry and biology have increasing in the past decade.[1–3] Vanadium is known to exist in a wide variety of oxidation states from −I to V, of which only vanadium(V), -(IV), and -(III) are biologically relevant. Vanadium(V) is an essential element of vanadium-dependent haloperoxidase found in marine algae and terrestrial fungi and of vanadium nitrogenase from *Azotobacter vinelandii*.[4] The vanadium(IV) species, named amavadin, has been found in the fly agaric toadstool *Amanita muscaria*.[5] Vanadium(IV) has been shown to have insulin mimetic functions.[6] Since Henze discovered that vanadium(III), which is an unstable oxidation state, accumulates in high levels in the blood cells of ascidians, known as tunicates or sea squirts, vanadium(III) species have been attracting the attention of chemists as well as biologists, though the function of vanadium(III) in ascidian blood cells has not yet been determined.[7–9] Interestingly, sulfate always co-exists with vanadium(III) in ascidian blood cells in spite of the fact that chloride is the most abundant anion in sea water. In order to obtain insight into the role of sulfate in tunicate blood cells, it is important to examine the coordination modes of sulfate to vanadium(III). In a previous paper, we reported the structures of vanadium(III) complexes in which the sulfate anion acted as a bidentate chelate ligand or a bridging ligand.[10] In this paper, we report the syntheses, structures, and properties of new dinuclear and tetranuclear vanadium(III) complexes containing alkoxo-bridging dinucleating ligand, 2-oxo-*N*,*N*′-bis(2-pyridylmethyl)-1,3-propanediamine-*N*,*N*′-diacetate (hpnbpda), and sulfato ligand. The vanadium(III)–hpnbpda complexes with a carboxylato bridge were also prepared to compare their properties with those of the sulfato-bridged complexes.

Experimental

Compound Preparations. Reagents were obtained from commercial sources and used without further purification. All of the synthetic procedures for vanadium(III) complexes were performed under an Ar atmosphere using standard Schlenk techniques or in a N_2-filled glove box.

***N*,*N*′-Bis(2-pyridylmethyl)-2-hydroxy-1,3-propanediamine-*N*,*N*′-diacetic Acid Hydrobromide Trihydrate (H_3hpnbpda·HBr·3H_2O).** H_3hpnbpda·HBr·3H_2O (Scheme 1) was prepared according to the literature method.[11]

$[\{V^{III}(H_2O)\}_2(\mu\text{-hpnbpda})(\mu\text{-OH})(\mu\text{-SO}_4)]\cdot 5.25H_2O$ (1). To an aqueous solution (20 cm^3) of anhydrous $V_2(SO_4)_3$[12] (1.2 g, 3.0 mmol) was added H_3hpnbpda·HBr·3H_2O (1.6 g, 3.0 mmol). Adjusting the pH of the solution to 3.5 by adding 1 mol dm^{-3} LiOH yielded a dark reddish brown solution. Dark red plates crystallized on standing at room temperature for one day. The crystals were collected by filtration, washed with cold water, and then dried. The crystals tend to effloresce and are oxidized on exposure to air. The crystals were, therefore, kept under Ar atmosphere. Yield 65%. Anal. Calcd for $C_{19}H_{36.5}N_4O_{17.25}SV_2 = [V_2(\text{hpnbpda})(OH)(SO_4)(H_2O)_2]\cdot 5.25H_2O$: C, 31.21; H, 5.04; N, 7.67%. Found: C, 31.48; H, 4.74; N, 7.77%. Selected IR data (KBr disk): 1653 (ν_{as}(COO)), 1484, 1445, 1383, 1335, 1307, 1245, 1192, 1166,

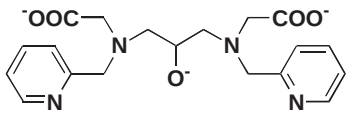

hpnbpda

Scheme 1.

Published on the web December 13, 2006; doi:10.1246/bcsj.79.1881

1117 ($\nu(SO_4)$), 1044 ($\nu(SO_4)$), 1027, 1006, 982, 964, 931, 771, 733, 701, 632 cm^{-1}.

$[V^{III}_4(\mu\text{-hpnbpda})_2(\mu\text{-OH})_2(\mu\text{-SO}_4)_2]\cdot 12H_2O$ (2). A dark reddish brown solution was obtained by the same procedure as shown above. The solution was concentrated to ca. 10 cm^3 by warming at 70 °C. Dark green plates crystallized on standing at 60 °C for a long period. The crystals were collected by filtration, washed with cold water, and then dried. Yield. 24%. Anal. Calcd for $C_{38}H_{68}N_8O_{32}S_2V_4 = [V_2(hpnbpda)_2(OH)_2(SO_4)_2]\cdot 12H_2O$: C, 32.21; H, 4.85; N, 7.91%. Found: C, 31.89; H, 4.67; N, 7.75%. Selected IR data (KBr disk): 1653 (ν_{as}(COO)), 1482, 1449, 1355, 1316, 1299, 1190, 1162, 1122 ($\nu(SO_4)$), 1039 ($\nu(SO_4)$), 999, 931, 861, 836, 777, 732, 680, 644, 604 cm^{-1}.

$[\{V^{III}(H_2O)\}_2(\mu\text{-hpnbpda})(\mu\text{-O}_2CC_2H_5)(\mu\text{-OH})]Br\cdot 7H_2O$ (3). A suspension containing anhydrous $V_2(SO_4)_3$ (0.8 g, 2.0 mmol) and $BaBr_2\cdot 2H_2O$ (2.1 g, 6.0 mmol) was warmed at 60 °C for 24 h to yield a solution of VBr_3. Barium sulfate precipitated was removed by filtration. To the filtrate was added an aqueous solution (20 cm^3) of H_3hpnbpda·HBr·$3H_2O$ (1.04 g, 2.0 mmol) and an excess amount of propionic acid (2 cm^3, ca. 40 mmol). The pH of the solution was adjusted to 3.5 by adding 1 mol dm^{-3} of LiOH. When this solution was evaporated, orange crystals were deposited. The crystals were re-dissolved in minimum amount of water by heating at 50 °C, and the resulting solution was allowed to stand at room temperature for three days. Orange plates were collected by filtration, washed with cold water, and then dried. The crystals tend to effloresce, and the complex is oxidized on exposure to air. The crystals were, therefore, kept under Ar atmosphere. Yield. 58%. Anal. Calcd for $C_{22}H_{45}N_4O_{17}BrV_2 = [V_2(hpnbpda)(O_2CC_2H_5)(OH)(H_2O)_2]Br\cdot 7H_2O$: C, 32.43; H, 5.32; N, 6.52%. Found: C, 32.24; H, 5.55; N, 6.84%. Selected IR data (KBr disk): 1629 (ν_{as}(COO), hpnbpda), 1557 (ν_{as}(COO), propionate), 1459, 1428, 1397, 1295, 1234, 1123, 1018, 996, 954, 926, 764, 723, 692, 566 cm^{-1}.

Measurements. UV–vis spectra were measured using a JASCO Ubest 50 spectrophotometer under argon atmosphere. Diffuse reflectance spectra were obtained for complexes diluted with MgO. Infrared spectra were recorded on a JASCO FT/IR-8000S. Since the vanadium(III) complexes obtained here are moderately stable to air oxidation in the solid state, the diffuse reflectance and infrared spectra were measured in air. The magnetic susceptibility was measured using the SQUID method on a Quantum Design MPMS-5S.

X-ray Structure Determination. The crystallographic data are summarized in Table 1. A crystal of $[\{V^{III}(H_2O)\}_2(\mu\text{-hpnbpda})(\mu\text{-OH})(\mu\text{-SO}_4)]\cdot 5.25H_2O$ (**1**) or $[V^{III}_4(\mu\text{-hpnbpda})_2(\mu\text{-OH})_2(\mu\text{-SO}_4)_2]\cdot 12H_2O$ (**2**) was mounted on a glass fiber, coated with epoxy resin as a precaution against solvent loss, and centered on a Rigaku AFC7S four-circle diffractometer (for **1**) or a Rigaku Mercury CCD system (for **2**) using graphite-monochromated Mo Kα radiation. Data reduction and the application of Lorentz, polarization, linear decay correction (for **1**), and empirical absorption corrections based on a series of ψ scans were carried out.

The structure was solved by direct methods, SIR97[13] for **1** and SHELX97[14] for **2**. Some remaining atom positions were found by successive Fourier techniques, DIRDIF99.[15] All of the non-hydrogen atoms were refined anisotropically. Hydrogen atoms were included but not refined. All calculations were performed using the CrystalStructure crystallographic software package.[16] Crystallographic data have been deposited with Cambridge Crystallographic Data Centre: Deposition numbers CCDC-616320 and CCDC-616321 for **1** and **2**, respectively. Copies of the data can be obtained free of charge via http://www.ccdc.cam.ac.uk/conts/retrieving.html (or from the Cambridge Crystallographic Data Centre, 12, Union Road, Cambridge, CB2 1EZ, UK; Fax: +44 1223 336033; e-mail: deposit@ccdc.cam.ac.uk).

Table 1. Crystallographic Data of $[\{V^{III}(H_2O)\}_2(\mu\text{-hpnbpda})(\mu\text{-SO}_4)(\mu\text{-OH})]\cdot 5.25H_2O$ (**1**) and $[V^{III}_4(\mu\text{-hpnbpda})_2(\mu\text{-SO}_4)_2(\mu\text{-OH})_2]\cdot 12H_2O$ (**2**)

	1	**2**
Formula	$C_{19}H_{36.5}N_4O_{17.25}SV_2$	$C_{38}H_{68}N_8O_{32}S_2V_4$
fw	730.96	1416.88
Temperature/K	296	296
λ(Mo Kα)/Å	0.71069	0.71069
Crystal system	triclinic	monoclinic
Space group	$P\bar{1}$	$P2_1/c$
a/Å	12.8868(5)	11.070(3)
b/Å	13.3741(5)	12.154(3)
c/Å	19.4059(9)	21.444(3)
α/deg	90.4059(11)	
β/deg	106.6966(11)	91.890(13)
γ/deg	108.0905(11)	
V/Å^3	2972.92(19)	2883.5(10)
Z	4	2
D_{calcd}/g cm^{-3}	1.633	1.632
μ/cm^{-1}	7.816	8.000
F(000)	1514	1464
No. of reflections		
Total	24359	6959
Unique	13392	6623
Observed ($I > 3\sigma(I)$)	11195	5246
No. of variables	826	400
R[a] ($I > 3\sigma(I)$)	0.045	0.056
Rw[b,c] ($I > 3\sigma(I)$)	0.085	0.099
GOF	1.004	1.003

a) $R = (\Sigma||F_o| - |F_c||)/\Sigma(|F_o|)$. b) $Rw = (\Sigma w(|F_o| - |F_c|)^2/\Sigma w(|F_o|^2)^{1/2}$. c) $w = 4(F_o)^2/s^2(F_o)$.

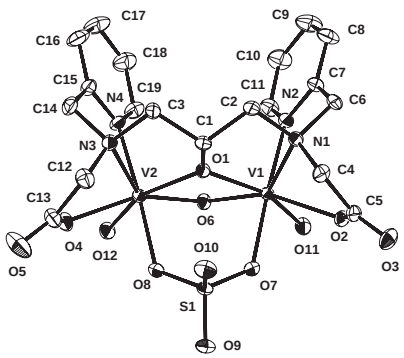

Fig. 1. Perspective view of $[\{V^{III}(H_2O)\}_2(\mu\text{-hpnbpda})(\mu\text{-OH})(\mu\text{-SO}_4)]$ (**1**).

Results and Discussion

X-ray Structures of $[\{V^{III}(H_2O)\}_2(\mu\text{-hpnbpda})(\mu\text{-OH})(\mu\text{-SO}_4)]\cdot 5.25H_2O$ (1) and $[V^{III}_4(\mu\text{-hpnbpda})_2(\mu\text{-OH})_2(\mu\text{-SO}_4)_2]\cdot 12H_2O$ (2). From the X-ray analysis, the unit cell of **1** contains two crystallographically independent complexes; however, their structures are almost the same. Figure 1 depicts the structure of one of the two complexes in the unit cell. Se-

Table 2. Selected Bond Distances (Å) and Angles (degree) for [{$V^{III}(H_2O)$}$_2$(μ-hpnbpda)(μ-SO_4)(μ-OH)]·5.25H_2O (**1**)

				Complex A			
V1–O1	2.006(2)	V2–O1	2.015(2)	O1–V1–O2	131.53(9)	O1–V2–O4	133.22(9)
V1–O2	2.100(2)	V2–O4	2.073(2)	O1–V1–O6	70.33(8)	O1–V2–O6	69.64(8)
V1–O6	1.988(2)	V2–O6	2.0135(19)	O1–V1–O7	85.75(7)	O1–V2–O8	85.69(8)
V1–O7	2.0993(15)	V2–O8	2.1016(18)	O1–V1–O11	150.79(9)	O1–V2–O12	148.52(8)
V1–O11	2.118(2)	V2–O12	2.109(2)	O1–V1–N1	73.61(8)	O1–V2–N3	73.15(9)
V1–N1	2.255(2)	V2–N3	2.265(2)	O1–V1–N2	98.96(8)	O1–V2–N4	98.57(9)
V1–N2	2.1505(19)	V2–N4	2.143(2)	O2–V1–O6	151.35(8)	O4–V2–O6	151.54(8)
V1⋯V2	3.2537(6)			O2–V1–O7	76.94(7)	O4–V2–O8	77.85(8)
				O2–V1–O11	75.52(9)	O4–V2–O12	76.07(8)
				O2–V1–N1	70.91(8)	O4–V2–N3	71.30(8)
				O2–V1–N2	101.84(8)	O4–V2–N4	99.86(9)
				O6–V1–O7	88.39(8)	O6–V2–O8	89.30(7)
				O6–V1–O11	80.52(8)	O6–V2–O12	79.01(8)
				O6–V1–N1	137.72(9)	O6–V2–N3	137.15(8)
				O6–V1–N2	90.36(9)	O6–V2–N4	91.11(8)
				O7–V1–O11	91.65(7)	O8–V2–O12	91.34(8)
				O7–V1–N1	110.34(8)	O8–V2–N3	108.47(8)
				O7–V1–N2	174.42(8)	O8–V2–N4	175.59(10)
				O11–V1–N1	133.67(8)	O12–V2–N3	136.63(10)
				O11–V1–N2	82.78(8)	O12–V2–N4	84.43(9)
				N1–V1–N2	74.07(9)	N3–V2–N4	74.06(9)
				Complex B			
V3–O13	2.012(2)	V4–O13	2.001(2)	O13–V3–O14	135.64(8)	O13–V4–O16	135.89(8)
V3–O14	2.072(2)	V4–O16	2.077(2)	O13–V3–O18	69.53(7)	O13–V4–O18	69.60(7)
V3–O18	1.995(2)	V4–O18	2.003(2)	O13–V3–O19	85.64(8)	O13–V4–O20	85.77(8)
V3–O19	2.094(2)	V4–O20	2.094(2)	O13–V3–O23	148.50(9)	O13–V4–O24	148.59(8)
V3–O23	2.1287(18)	V4–O24	2.133(2)	O13–V3–N5	73.20(9)	O13–V4–N7	73.86(9)
V3–N5	2.267(2)	V4–N7	2.254(2)	O13–V3–N6	96.97(9)	O13–V4–N8	94.90(10)
V3–N6	2.146(2)	V4–N8	2.142(2)	O14–V3–O18	149.86(7)	O16–V4–O18	148.55(7)
V3⋯V4	3.2553(7)			O14–V3–O19	78.35(9)	O16–V4–O20	77.67(10)
				O14–V3–O23	74.45(9)	O16–V4–O24	74.66(8)
				O14–V3–N5	71.45(8)	O16–V4–N7	71.43(8)
				O14–V3–N6	98.72(10)	O16–V4–N8	101.34(11)
				O18–V3–O19	89.76(9)	O18–V4–O20	88.61(9)
				O18–V3–O23	78.97(9)	O18–V4–O24	79.16(9)
				O18–V3–N5	138.68(9)	O18–V4–N7	139.93(9)
				O18–V3–N6	92.52(9)	O18–V4–N8	92.31(10)
				O19–V3–O23	94.12(8)	O20–V4–O24	96.88(8)
				O19–V3–N5	104.70(8)	O20–V4–N7	104.70(8)
				O19–V3–N6	177.00(11)	O20–V4–N8	179.00(11)
				O23–V3–N5	136.34(10)	O24–V4–N7	134.29(10)
				O23–V3–N6	84.42(8)	O24–V4–N8	82.93(9)
				N5–V3–N6	74.77(8)	N7–V4–N8	74.81(9)

lected bond distances and angles are summarized in Table 2. Complex **1** is a dinuclear vanadium(III) complex triply bridged by a deprotonated alkoxo group of hpnbpda, a hydroxo group, and a sulfato group. Taking into account the charge balance in **1**, we concluded that the bridging group is a hydroxo, not an oxo ligand. A similar triply bridged structure has been found for [{$V^{III}(H_2O)$}$_2$(μ-bza)(μ-OH)(μ-tphpn)]$^{3+}$ (bza: benzoate; tphpn: 2-oxo-*N*,*N*,*N*′,*N*′-tetra(2-pyridylmethyl)-1,3-propanediamine), in which a benzoate group bridges two vanadium(III) ions instead of a sulfato group.[11] The two pyridylmethyl groups (and thus the two acetate groups) of hpnbpda are located on the same side, and thus, the complex has a quasi-mirror plane through atoms C1, O1, O6, and S1. As a consequence, the two asymmetric nitrogen atoms have an opposite absolute configuration with each other (namely, a meso form). Each vanadium(III) center has a heptacoordinate geometry. Heptacoordination is not unusual for vanadium(III) complexes and has been found in several complexes containing a multidentate ligand, such as K[V^{III}(edta)(H_2O)],[17] K[V^{III}(cydta)(H_2O)],[18] [V^{III}(nta)(H_2O)$_3$],[19] K_2[V^{III}_2(μ-Hdpot)$_2$] (dpot: 2-oxo-1,3-propanediamine-*N*,*N*,*N*′,*N*′-tetraacetate),[20] [V^{III}_2(μ-hpnbpda)$_2$],[11] and [{$V^{III}(H_2O)$}$_2$(μ-bza)(μ-OH)(μ-tphpn)]Cl_3.[11] The idealized coordination polyhedrons for heptacoordinated complexes can be classified into three forms: a pentagonal bipyramid, a

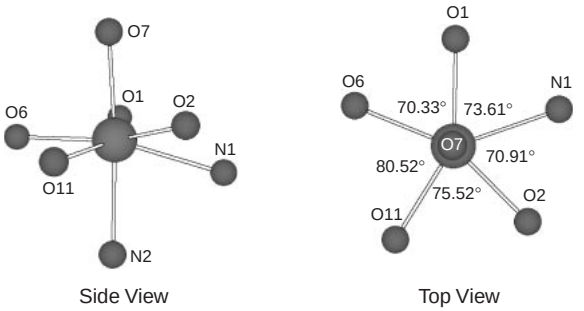

Fig. 2. Side and top views of the coordination polyhedron in **1**.

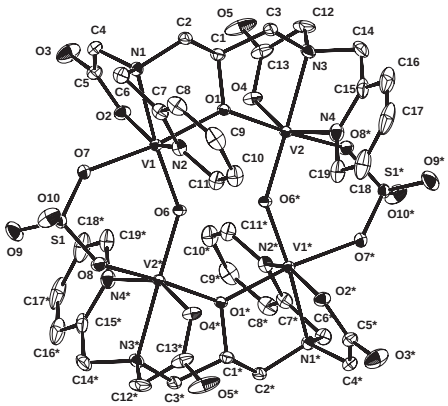

Fig. 3. Perspective view of $[V^{III}{}_4(\mu\text{-hpnbpda})_2(\mu\text{-OH})_2(\mu\text{-SO}_4)_2]$ (**2**).

capped octahedron, and a capped trigonal prism. However, the real complex usually adopts an intermediate structure. From Fig. 2, the coordination polyhedron of the present complex is a pentagonal bipyramid, which is different from that found in the related triply bridged complex $[\{V^{III}(H_2O)\}_2(\mu\text{-bza})(\mu\text{-OH})(\mu\text{-tphpn})]^{3+}$, which had a capped octahedron[11] but is similar to that found in $[V^{III}{}_2(\mu\text{-hpnbpda})_2]$.[11] Atoms O1 (alkoxo oxygen), N1 (amino nitrogen), O2 (carboxylato oxygen), O11 (aqua oxygen), and O6 (hydroxo oxygen) complete the pentagonal plane, and atoms N2 (pyridyl nitrogen) and O7 (sulfato oxygen) occupy the axial positions. However, the pentagonal bipyramid adopted by **1** is fairly distorted from ideal geometry as shown in Fig. 2.

It is of interest to compare the bond distances in the present complex with those of the related triply bridged complex, $[\{V^{III}(H_2O)\}_2(\mu\text{-bza})(\mu\text{-OH})(\mu\text{-tphpn})]^{3+}$,[11] though the coordination polyhedrons are different with each other as mentioned above. The V–O(alkoxo), V–O(hydroxo), V–O(aqua), and V–N(amine) distances agree within 0.035 Å. However, the V–N(pyridine) distance in complex **1** (av. 2.147 Å) is a little bit shorter than the corresponding one in the latter complex (av. 2.231 Å).

A perspective view of **2** is shown in Fig. 3, and selected bond distances and angles are summarized in Table 3. Two dinuclear vanadium(III) units bridged by the alkoxo group of hpnbpda are further linked by the two hydroxo and the two sulfato bridging groups, resulting in a tetranuclear structure (so-called dimer-of-dimers). The tetranuclear unit has a center of symmetry. A similar dimer-of-dimers structure has been found for iron[21,22] and manganese[23,24] complexes with an alkoxo-bridging dinucleating ligand. Interestingly, each vanadium(III) center has a hexacoordinate structure, which is different from the heptacoordinate structure found in the dinuclear hpnbpda complex **1**. The terminal terdentate moiety of hpnbpda coordinates to vanadium(III) center in a meridional fashion bringing about a highly distorted octahedron, which is represented by small trans angles of O2–V1–N2 (154.15(12)°) and O4–V2–N4 (153.26(13)°). The coordination mode (meridional or facial) of the terminal terdentate moiety of an alkoxo-bridging dinucleating ligand seems to depend on the arrangement of other bridging groups.[21–24]

Table 3. Selected Bond Distances (Å) and Angles (degree) for $[V^{III}{}_4(\mu\text{-hpnbpda})_2(\mu\text{-OH})_2(\mu\text{-SO}_4)_2]\cdot 12H_2O$ (**2**)[a)]

V1–O1	2.042(2)	V2–O1	2.036(2)
V1–O2	1.984(2)	V2–O4	1.988(2)
V1–O6	1.871(2)	V2–O6*	1.888(2)
V1–O7	2.040(3)	V2–O8*	2.046(3)
V1–N1	2.174(3)	V2–N3	2.175(3)
V1–N2	2.118(3)	V2–N4	2.111(3)
V1···V2	3.7436(8)	V1···V2*	3.5320(7)
O1–V1–O2	89.64(10)	O1–V2–O4	88.66(10)
O1–V1–O6	93.14(10)	O1–V2–O6*	91.83(10)
O1–V1–O7	173.14(10)	O1–V2–O8*	173.97(10)
O1–V1–N1	83.22(10)	O1–V2–N3	82.63(11)
O1–V1–N2	90.19(11)	O1–V2–N4	93.52(12)
O2–V1–O6	107.20(11)	O4–V2–O6*	108.28(11)
O2–V1–O7	85.77(12)	O4–V2–O8*	85.71(11)
O2–V1–N1	78.76(11)	O4–V2–N3	78.38(12)
O2–V1–N2	154.15(12)	O4–V2–N4	153.26(13)
O6–V1–O7	93.09(11)	O6*–V2–O8*	91.98(11)
O6–V1–N1	173.07(11)	O6*–V2–N3	171.32(13)
O6–V1–N2	98.63(12)	O6*–V2–N4	98.30(12)
O7–V1–N1	90.87(11)	O8*–V2–N3	94.11(12)
O7–V1–N2	91.71(13)	O8*–V2–N4	90.55(13)
N1–V1–N2	75.55(12)	N3–V2–N4	75.49(13)

a) Symmetry operators: $-X+1$, $-Y+1$, $-Z+1$.

The coordination bond distances in **2** are shorter than the corresponding ones in **1**, reflecting a decrease of the coordination number. The alkoxo bridging angle, V1–O1–V2 in **2** (133.25(11)°) is rather large compared to that in **1** (av. 108.22°). Thus, the small alkoxo bridging angle in **1** must be a consequence of the triple bridge. The hydroxo bridging angle, V1–O6–V2* (139.95(14)°) and the V–O–S angles (av. 136.84°) in **2** are also large compared to those in **1** (108.82(9)° and av. 129.61°, respectively). The O–S–O angles are rigid, and they do not differ so much in **1** and **2**: the average angle is 109.5° for both complexes. The V···V distances are in the order of V1···V2 in **1** (av. 3.2543 Å) < V1···V2* in **2** (3.5320(7) Å) < V1···V2 in **2** (3.7436(8) Å), reflecting the number of bridging groups, i.e., 3, 2, and 1, respectively.

All of the waters of crystallization in **1** and **2** were found to take part in hydrogen bonding. The O···O contacts within 3 Å are summarized in Table 4. The carboxylate oxygen atoms and the sulfate oxygen atoms in **1** and **2**, as well as the aqua ligand in **1**, are all linked by a hydrogen bond to the waters of crystallization. The hydrogen bonds between the water molecules of crystallization also exist.

Table 4. Various Types of Hydrogen Bond (within 3 Å) Involving Water of Crystallization for **1** and **2**

Type[a)]	**1**		**2**	
$O_w \cdots O_{carbox,\,u}$	O25···O5	2.743(4)	O11···O3	2.763(6)
	O26···O3	2.756(4)	O16···O5	2.866(8)
	O26···O15	2.653(3)		
	O29···O17	2.856(4)		
	O33···O5	2.800(5)		
	O33···O17	2.897(4)		
	O34···O15	2.755(5)		
$O_w \cdots O_{carbox,\,c}$	O27···O2	2.801(3)	O14···O2	2.949(7)
	O31···O14	2.924(4)	O14···O4	2.895(7)
	O31···O16	2.839(4)		
$O_w \cdots O_{sulfate,\,u}$	O28···O9	2.802(4)	O11···O9	2.884(6)
	O28···O22	2.944(3)	O15···O10	2.897(7)
	O30···O21	2.859(4)		
	O35···O10	2.969(10)		
$O_w \cdots O_{aq}$	O26···O11	2.717(3)		
	O27···O12	2.679(3)		
	O29···O24	2.778(5)		
	O31···O23	2.986(6)		
	O33···O23	2.992(5)		
$O_w \cdots O_w$	O25···O26	2.722(4)	O12···O13	2.827(9)
	O25···O27	2.827(4)	O12···O16	2.794(8)
	O25···O30	2.836(5)	O14···O15	2.818(9)
	O28···O32	2.834(5)		
	O29···O34	2.815(7)		
	O32···O34	2.800(8)		

a) O_w: water of crystallization, $O_{carbox,\,u}$: uncoordinated carboxylate oxygen, $O_{carbox,\,c}$: coordinated carboxylate oxygen, $O_{sulfate,\,u}$: uncoordinated sulfate oxygen, O_{aq}: aqua ligand.

Estimation of the Structures of the Carboxylato-Bridging Complexes, [{$V^{III}(H_2O)$}$_2$(μ-hpnbpda)(μ-$O_2CC_2H_5$)(μ-OH)]Br·$7H_2O$ (3) and [{$V^{III}(H_2O)$}$_2$(μ-hpnbpda)(μ-$O_2CC_6H_5$)]Cl_2·$2H_2O$ (4). Two carboxylato (propionato and benzoato) bridging complexes were prepared in order to compare the properties with those of the sulfato-bridging complexes. Preparation of a complex with an acetato bridge was also tried; however, it could not be isolated due to poor crystallinity. Although the preparation of **4** has been reported in an earlier paper,[11] its structure was discussed only very briefly. The structure of **4** will be estimated here in comparison with that of **3**.

Since we could not obtained X-ray quality of crystals of **3** and **4**, the structures of the carboxylato-bridging complexes were estimated on the basis of their elemental analyses, IR spectra, and UV–vis spectra. From elemental analysis and charge balance considerations, complex **3** consists of two vanadium(III) ions, one hpnbpda ligand, one propionate, one hydroxide, one bromide, and nine water molecules, and complex **4** consists of two vanadium(III) ions, one hpnbpda ligand, one benzoate, two chloride, and four water molecules.

The IR spectra of **3** and **4** are shown in Fig. 4. A carboxylate anion can coordinate to metal ion as an unidentate ligand, a bidentate ligand, or a bridging ligand. The COO stretching vibrations are diagnostic for the coordination modes.[25] Although the difference between the two COO stretching modes (ν_{as}(COO) − ν_s(COO)) has been considered to be the most reliable diagnosis, unambiguous assignment of the ν_s(COO) of the present complexes was difficult because of the complexity of the IR spectrum in the region of 1300–1500 cm^{-1}, in which the ν_s(COO) is expected to appear. However, the following facts indicate that the complexes **3** and **4** contain a bridging carboxylato group: (1) the ν_{as}(COO) generally appears around 1550 cm^{-1} for bridging carboxylate ions whereas it appears above 1600 cm^{-1} for terminal carboxylate ions; (2) complexes **3** and **4** exhibit intense bands at 1557 and 1537 cm^{-1}, respectively, which can be assigned to the ν_{as}(COO) of a bridging carboxylato group, in addition to bands at 1629 and 1654 cm^{-1} due to the ν_{as}(COO) of the terminal carboxylato group of the hpnbpda ligand; (3) complexes **3** and **4** contain only one propionate or benzoate ion per dimeric unit.

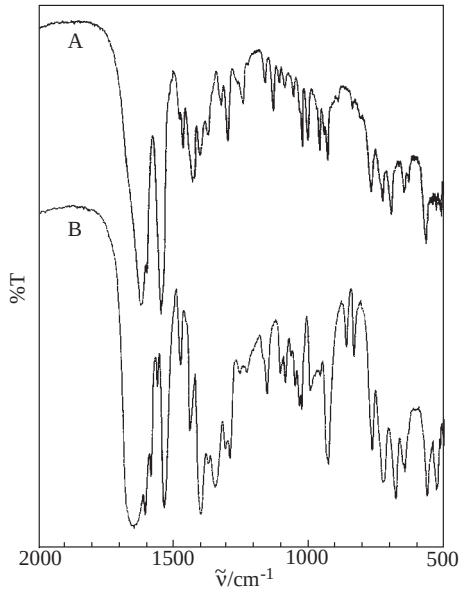

Fig. 4. Infrared spectra of **3** (A) and **4** (B).

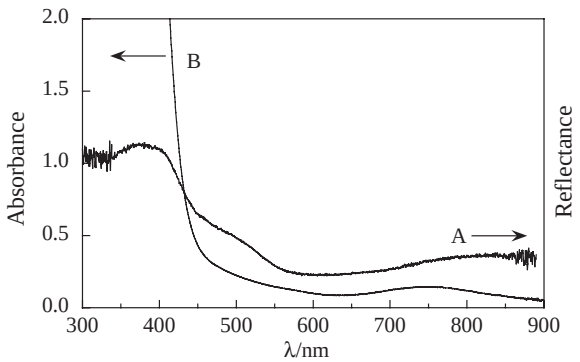

Fig. 5. Diffuse reflectance and absorption spectra of **3**: A, diffuse reflectance spectrum; B, absorption spectrum in EtOH (5.0 mmol dm^{-3}/V).

Figure 5A shows a diffuse reflectance spectrum of the complex **3**. It is known that heptacoordinate vanadium(III) complexes exhibit an absorption bands around 800 nm while the

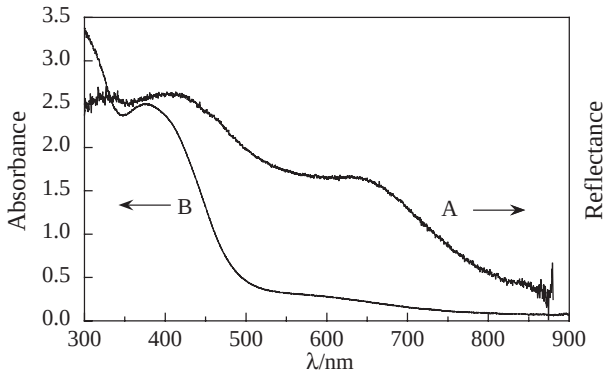

Fig. 6. Diffuse reflectance and absorption spectra of **4**: A, diffuse reflectance spectrum; B, absorption spectrum in DMSO (1.0 mmol dm^{-3}/V).

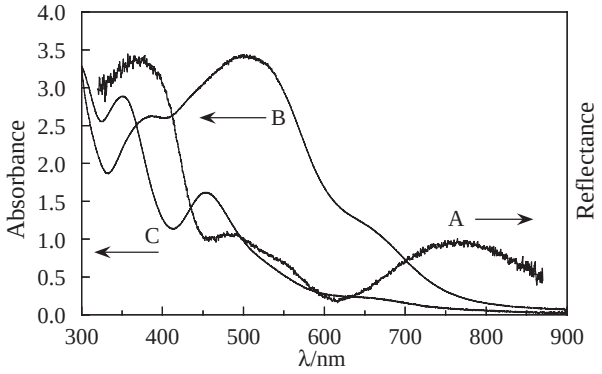

Fig. 7. Diffuse reflectance and absorption spectra of **1**: A, diffuse reflectance spectrum; B, absorption spectrum in DMSO (5.0 mmol dm^{-3}/V); C, absorption spectrum in water (2.5 mmol dm^{-3}/V).

band is absent for hexacoordinate complexes.[20,26] The broad band around 800 nm observed for complex **3**, thus, indicates a heptacoordinate structure. Taking this into consideration, complex **3** most likely has a heptacoordinate structure, bridged by an alkoxo group of hpnbpda, a propionato group, and a hydroxo group, and can be formulated as $[\{V^{III}(H_2O)\}_2(\mu\text{-hpnbpda})(\mu\text{-}O_2CC_2H_5)(\mu\text{-OH})]Br\cdot 7H_2O$. A similar structure has been found for $[\{V^{III}(H_2O)\}_2(\mu\text{-}O_2CC_6H_5)(\mu\text{-OH})(\mu\text{-tphpn})]Cl_3$.[11,27]

A diffuse reflectance spectrum of the complex **4** is shown in Fig. 6A. In contrast to the spectrum of **3**, that of **4** lacks a band characteristic to a heptacoordination around 800 nm, indicating that **4** adopts a hexacoordinate structure. Thus, complex **4** can be formulated as $[\{V^{III}(H_2O)\}_2(\mu\text{-hpnbpda})(\mu\text{-}O_2CC_6H_5)]Cl_2\cdot 2H_2O$. A similar coordination environment has been found in $[\{V^{III}(H_2O)\}_2(\mu\text{-dpot})(\mu\text{-}m\text{-hbza})]$ (*m*-hbza is *meta*-hydroxybenzoate).[28] Interestingly, the hpnbpda ligand, which has an intermediate structure of tphpn and dpot, yields heptacoordinate as well as hexacoordinate dinuclear vanadium(III) complexes found for the tphpn and dpot complexes, respectively, depending on the carboxylate ions employed as a second bridging group.

Preparation of the hpnbpda Complexes. It is appropriate to mention here the general view toward the preparation of the vanadium(III) complexes with hpnbpda. We have prepared five different types of vanadium(III)–hpnbpda complexes including $[\{V^{III}(H_2O)\}_2(\mu\text{-hpnbpda})(\mu\text{-bza})]Cl_2$ (**4**) and $[V^{III}{}_2(\mu\text{-hpnbpda})_2]$ reported earlier.[11] The composition and the structure of the complexes deposited from the reaction solution seem to depend on the nature of the additional bridging ligand and the anion in the reaction. The pH and the concentration of the reaction solution and the crystallizing temperature also affect the structure of the complex. $[V^{III}{}_2(\mu\text{-hpnbpda})_2]$ was found to be easiest to crystallize in the absence of the additional bridging ligand. In fact, this complex often precipitated simultaneously with the other complexes. Controlling the pH of the reaction solution seems to be an important factor to obtain the desired complex.

The sulfato-bridging complexes **1** and **2** could be crystallized separately by regulating both the concentration and the temperature of the reaction mixture, from which the crystals were grown. Namely, the tetranuclear complex **2** was isolated from a concentrated solution at a higher crystallizing temperature (60 °C vs room temperature for the dinuclear complex). It is conceivable that concentrating the solution makes the formation of the complex with a higher nuclearity more favorable. The dinuclear and tetranuclear structures of the vanadium(III)–hpnbpda–SO_4^{2-} complexes seem to be formed by so-called "spontaneous self-assembly" on crystallization.

The choice of counter ion may more or less contribute to the structure of vanadium(III)–hpnbpda complexes. We used bromide instead of chloride in the preparation of **3**. It is not clear, at present, if the heptacoordinate structure of **3** is the result of using bromide as a counter ion, since the corresponding chloride was not obtained due to its low crystallinity.

Structures in Solution. Since vanadium(III) complexes are substitutionally labile, the structures found in the solid states are not necessarily kept intact in solutions. In order to know if the solid-state structure is maintained in solution, the absorption spectra of **1** and **2** in DMSO were compared with those of the diffuse reflectance spectra. The diffuse reflectance spectrum of **1** (Fig. 7, spectrum A) exhibits the band at 780 nm characteristic of heptacoordination, which is consistent with the X-ray structure. However, this 780-nm band disappeared in DMSO, and the spectral feature was completely different from that in the solid state (spectrum B). This fact suggests that the sulfato or hydroxo bridge is decomposed in DMSO to yield a hexacoordinate species. Since the hexa- and heptacoordinate species would be expected to have a rather different stability with each other, it is not likely that these two species coexist at equilibrium in DMSO. In water, **1** exhibited a different spectral feature from those obtained in the solid state as well as in DMSO (see spectrum C). Although this spectral change may indicate that another type of decomposition occurred in water, we will not consider further the structure of the complex in water since the structure of the substitutionally labile complex depends on its concentration and temperature, and especially on the pH in water.

Figure 8 shows the absorption spectrum and the diffuse reflectance spectrum of **2**. In this case, the absorption spectrum in DMSO corresponds well to the diffuse reflectance spectrum, suggesting the solid-state structure is kept intact in DMSO. This is distinct from the behavior of **1**, indicating that the tetra-

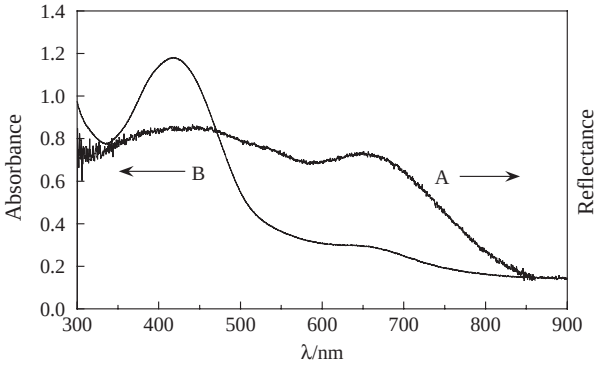

Fig. 8. Diffuse reflectance and absorption spectra of **2**: A, diffuse reflectance spectrum; B, absorption spectrum in DMSO (1.0 mmol dm^{-3}/V).

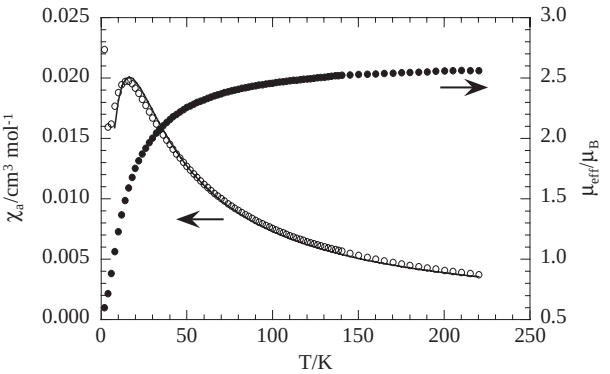

Fig. 9. Plot of the magnetic susceptibility and the effective magnetic moment against temperature for **1**.

nuclear structure would be less strained as a whole than the dinuclear one. The small V–O(alkoxo)–V and V–O(hydroxo)–V angles in **1** compared with those in **2** may be a reason for the strain.

The absorption spectrum of **3** in ethanol is shown in Fig. 5B. A DMSO solution exhibited a similar spectrum. The 780-nm band indicates that heptacoordination is kept in ethanolic and DMSO solutions. The blue shift of the bands compared with the solid-state spectrum may be due to a solvent effect. Figure 6B shows the absorption spectrum of **4** in DMSO. Although a blue shift was also observed, the spectrum in DMSO corresponds well to that in the solid state, suggesting that the coordination environment in the solid state is maintained in DMSO. In other words, the carboxylato-bridged dinuclear vanadium(III) complexes are more stable at least in DMSO than the corresponding sulfato-bridged complex (**1**).

Magnetic Properties. Dinuclear vanadium(III) complexes show a variety of intramolecular spin-exchange coupling from a strong ferromagnetic coupling to a strong antiferromagnetic coupling, depending on the bridging mode.[9] We studied the magnetic properties of complexes **1** and **2**, of which structures were determined by X-ray crystallography. Figure 9 shows the magnetic susceptibility (χ_a/V) and the effective magnetic moment (μ_{eff}/V) of **1** as a function of temperature in the region of 2 to 300 K. The effective magnetic moment at 300 K is 2.56 μ_B, which is comparable to that expected for a magnetically isolated V^{III} (d^2) ion (2.83 μ_B). The μ_{eff} decreases with decreasing temperature, indicating antiferromagnetic coupling. The temperature dependence of the magnetic susceptibility was analyzed on the basis of the spin-Hamiltonian $H = -2JS_1 \cdot S_2$ ($S_1 = S_2 = 1$). Temperature-independent paramagnetism was neglected in the calculation. The rapid increase in χ_a below 6 K may be due to a paramagnetic impurity and those data were omitted in the calculation. A least-squares fit to the experimental data, given as a solid line in Fig. 9, yielded $J = -5.9\,cm^{-1}$ and $g = 1.90$. The J value of **1** is comparable to that obtained for the heptacoordinate di(alkoxo)-bridged dinuclear vanadium(III) complex, $[V^{III}{}_2(\mu\text{-Hhedtra})_2]^{2-}$ (Hhedtra = *N*-hydroxyethyl-1,2-ethanediamine-*N*,*N*′,*N*′-triacetate) ($J = -8.6\,cm^{-1}$).[29]

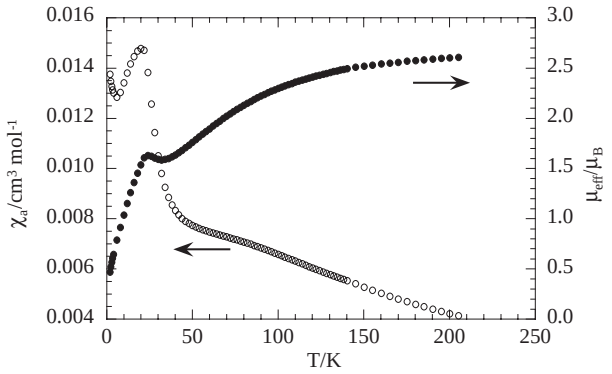

Fig. 10. Plot of the magnetic susceptibility and the effective magnetic moment against temperature for **2**.

The temperature dependence of χ_a and μ_{eff} for **2** exhibited a complex feature (Fig. 10). The μ_{eff} at 300 K (2.61 μ_B) also corresponds to that expected for a magnetically isolated V^{III} (d^2) ion. The μ_{eff} decreased gradually from 300 to 50 K and then slightly increased followed by a rapid decrease. Although we tried to reproduce the temperature dependence of the magnetic susceptibility, including the coupling constant of the alkoxo-bridging moiety ($J_{12} = J_{1*2*}$) and that of the sulfato- and hydroxo-bridging moiety ($J_{12*} = J_{1*2}$), as well as a space-through coupling constant ($J_{11*} = J_{22*}$), a satisfactory fit could not be obtained so far using spin-Hamiltonian $H = -2J_{12}S_1 \cdot S_2 - 2J_{1*2*}S_{1*} \cdot S_{2*} - 2J_{12*}S_1 \cdot S_{2*} - 2J_{1*2}S_{1*} \cdot S_2 - 2J_{11*}S_1 \cdot S_{1*} - 2J_{22*}S_2 \cdot S_{2*}$ (the numbering scheme corresponds to the crystallographic numbering for V atoms in Fig. 3).

In conclusion, it was found that an alkoxo-bridging dinucleating ligand, hpnbpda, yields a variety of multinuclear vanadium(III) complexes mainly depending on the nature of additional bridging ligands and the crystallization conditions. Namely, $[V^{III}{}_2(\mu\text{-hpnbpda})_2]$ is preferentially formed when an additional bridging ligand is absent.[11] When the carboxylates were used as an additional bridging ligand, the hexacoordinate dinuclear complex doubly bridged by hpnbpda and a carboxylate (**4**) or the heptacoordinate dinuclear complex triply bridged by hpnbpda, a carboxylate, and an extra hydroxo group (**3**) were obtained, probably depending on the nature of the carboxylate ligand used. Sulfato group can also function as a bridging ligand. The heptacoordinate dinuclear complex (**1**) and hexacoordinate tetranuclear complex (**2**) were obtained separately by controlling the crystallization condition.

We are very grateful to Prof. Wasuke Mori of Kanagawa University for his help in the measurement of the magnetic susceptibility and a useful discussion with him.

References

1 *Vanadium and Its Role in Life* in *Metal Ions in Biological Systems*, ed. by H. Sigel, A. Sigel, Marcel Dekker, New York, **1995**, Vol. 31.

2 *Vanadium in the Environment* in *Advances in Environmental Science and Technology*, ed. by J. O. Nriagu, John Wiley & Sons, New York, **1998**, Vol. 30.

3 Special Issue: New Direction in Chemistry and Biological Chemistry of Vanadium. *Coord. Chem. Rev.* **2003**, *237*.

4 R. Wever, W. Hemrika, *Vanadium in the Environment, Part 1* in *Advances in Environmental Science and Technology*, ed. by J. O. Nriagu, John Wiley & Sons, New York, **1998**, Vol. 30, pp. 285–305.

5 E. Bayer, E. Koch, G. Anderegg, *Angew. Chem., Int. Ed. Engl.* **1987**, *26*, 545.

6 H. Sakurai, A. Tsuji, *Vanadium in the Environment, Part 2* in *Advances in Environmental Science and Technology*, ed. by J. O. Nriagu, John Wiley & Sons, New York, **1998**, Vol. 30, pp. 297–315.

7 M. Henze, *Hoppe-Seyler's Z. Physiol. Chem.* **1911**, *72*, 494.

8 H. Michibata, N. Yamaguchi, T. Uyama, T. Ueki, *Coord. Chem. Rev.* **2003**, *237*, 41.

9 K. Kanamori, *Coord. Chem. Rev.* **2003**, *237*, 147.

10 K. Kanamori, E. Kameda, K. Okamoto, *Bull. Chem. Soc. Jpn.* **1996**, *69*, 2901.

11 K. Kanamori, K. Yamamoto, T. Okayasu, N. Matsui, K. Okamoto, W. Mori, *Bull. Chem. Soc. Jpn.* **1997**, *70*, 3031.

12 J. C. Claunchi, M. M. Jones, *Inorg. Synth.* **1963**, *7*, 92.

13 A. Altomare, M. Burla, M. Camalli, G. Cascarano, C. Giacovazzo, A. Guagliardi, A. Moliterni, G. Polidori, R. Spagna, *J. Appl. Crystallogr.* **1999**, *32*, 115.

14 G. M. Sheldrick, *SHELX97 Program for Crystal Structure Refinement from Diffraction Data*, University of Göttingen, Göttingen, Germany, **1997**.

15 P. T. Beurskens, G. Admiraal, G. Beurskens, W. P. Bosman, R. de Gelder, R. Israel, J. M. M. Smits, *The DIRDIF-99 Program System, Technical Report on the Crystallography Laboratory*, University of Nijmergen, The Netherlands, **1999**.

16 CrystalStructure 3.7.0: Crystal Structure Analysis Package, Rigaku and Rigaku/MSC, **2000–2005**. 9009 New Trails Dr. The Woodlands TX 77381 U.S.A.

17 M. Shimoi, Y. Saito, H. Ogino, *Chem. Lett.* **1989**, 1675.

18 M. Shimoi, S. Miyamoto, H. Ogino, *Bull. Chem. Soc. Jpn.* **1991**, *64*, 2549.

19 K. Okamoto, J. Hidaka, M. Fukagawa, K. Kanamori, *Acta Crystallogr., Sect. C* **1992**, *48*, 1025.

20 J. C. Robles, Y. Matsuzaka, S. Inomata, M. Shimoi, W. Mori, H. Ogino, *Inorg. Chem.* **1993**, *32*, 13.

21 D. L. Jameson, C. L. Xie, D. N. Hendrickson, J. A. Potenza, H. J. Schugar, *J. Am. Chem. Soc.* **1987**, *109*, 740.

22 S. Yano, T. Inagaki, Y. Yamada, M. Kato, M. Yamasaki, K. Sakai, T. Tsubomura, M. Sato, W. Mori, K. Yamaguchi, I. Kinoshita, *Chem. Lett.* **1996**, 61.

23 R. T. Stibrany, S. M. Gorun, *Angew. Chem., Int. Ed. Engl.* **1990**, *29*, 1156.

24 M. L. Kirk, M. K. Chen, W. H. Armstrong, E. I. Solomon, *J. Am. Chem. Soc.* **1992**, *114*, 10432.

25 K. Nakamoto, *Infrared and Raman Spectra of Inorganic and Coordination Compounds, Part B*, 5th ed., John Wiley & Sons, New York, **1997**, pp. 59–62.

26 K. Kanamori, K. Ino, H. Maeda, K. Miyazaki, M. Fukagawa, J. Kumada, T. Eguchi, K. Okamoto, *Inorg. Chem.* **1994**, *33*, 5547.

27 K. Kanamori, T. Okayasu, K. Okamoto, *Chem. Lett.* **1995**, 105.

28 K. Kanamori, K. Yamamoto, K. Okamoto, *Chem. Lett.* **1993**, 1253.

29 T. K. Shepherd, W. E. Hatfield, D. Ghosh, C. D. Stout, F. J. Kristine, J. R. Ruble, *J. Am. Chem. Soc.* **1981**, *103*, 5511.